The beta 2-adrenergic receptor as a surrogate odorant receptor in mouse olfactory sensory neurons

Masayo Omura, Xavier Grosmaitre, Minghong Ma, Peter Mombaerts

Molecular and Cellular Neuroscience 58 (2014) 1–10

Contents lists available at ScienceDirect

Molecular and Cellular Neuroscience

journal homepage: www.elsevier.com/locate/ymcne

The β2-adrenergic receptor as a surrogate odorant receptor in mouse olfactory sensory neurons

Masayo Omura [a], Xavier Grosmaitre [b,c], Minghong Ma [b], Peter Mombaerts [a,*]

[a] Max Planck Research Unit for Neurogenetics, Max-von-Laue-Strasse 3, 60438 Frankfurt, Germany
[b] Department of Neuroscience, University of Pennsylvania School of Medicine, Philadelphia, PA 19104, USA
[c] Centre des Sciences du Goût et de l'Alimentation, 21000 Dijon, France

ARTICLE INFO

Article history:
Received 12 September 2013
Revised 9 October 2013
Accepted 29 October 2013
Available online 6 November 2013

Keywords:
Main olfactory epithelium
Odorant receptor
β2-adrenergic receptor
G-protein coupled receptor

ABSTRACT

In the mouse, mature olfactory sensory neurons (OSNs) express one allele of one of the ~1200 odorant receptor (OR) genes, which encode G-protein coupled receptors (GPCRs). Axons of OSNs that express the same OR coalesce into homogeneous glomeruli at conserved positions in the olfactory bulb. ORs are involved in OR gene choice and OSN axonal wiring, but the mechanisms remain poorly understood. One approach is to substitute an OR genetically with another GPCR, and to determine in which aspects this GPCR can serve as a surrogate OR under experimental conditions. Here, we characterize a novel gene-targeted mouse strain in which the mouse β2-adrenergic receptor (β2AR) is coexpressed with tauGFP in OSNs that choose the OR locus *M71* for expression (β2AR→M71-GFP). By crossing these mice with β2AR→M71-lacZ gene-targeted mice, we find that differentially tagged β2AR→M71 alleles are expressed monoallelically. The OR coding sequence is thus not required for monoallelic expression — the expression of one of the two alleles of a given OR gene in an OSN. We detect strong β2AR immunoreactivity in dendritic cilia of β2AR→M71-GFP OSNs. These OSNs respond to the β2AR agonist isoproterenol in a dose-dependent manner. Axons of β2AR→M71-GFP OSNs coalesce into homogeneous glomeruli, and β2AR immunoreactivity is detectable within these glomeruli. We do not find evidence for expression of endogenous β2AR in OSNs of wild-type mice, also not in M71-expressing OSNs, and we do not observe overt differences in the olfactory system of β2AR and β1AR knockout mice. Our findings corroborate the experimental value of the β2AR as a surrogate OR, including for the study of the mechanisms of monoallelic expression.

Introduction

There is still a lack of mechanistic understanding of two fundamental and striking features of mouse olfactory sensory neurons (OSNs). First, each mature OSN expresses one allele of one gene of the ~1200 OR genes (Buck and Axel, 1991) that are scattered over more than 40 loci in the genome. The features of monoallelic expression (one of two alleles of an OR gene per OSN) and monogenic expression (one OR gene per OSN) may or may not be governed by the same regulatory mechanisms. Second, axons from OSNs that express the same OR gene coalesce during development into one or a few homogeneous glomeruli in the medial and lateral halves of the olfactory bulb (Mombaerts et al., 1996). These glomeruli reside at conserved positions. The molecular and cellular mechanisms of OR gene choice and OR-specific axonal coalescence into glomeruli remain poorly understood. The models and hypotheses that have been formulated involve the ORs themselves, but it is not clear or has not been addressed to which extent these properties are specific to ORs. Conceivably, ORs may have evolved unique functions in certain aspects of OR gene choice and OSN axonal wiring. In other aspects, other GPCRs (non-olfactory GPCRs) may be able to serve as surrogates for ORs under experimental conditions, such as when expressed in an OR-like fashion. Of particular interest are the non-olfactory GPCRs that can couple to $G_{\alpha}olf$ or $G_{\alpha}s$, the G protein subunits to which ORs couple normally within OSNs. Relatively little is known about structure–function relationships of ORs, but other GPCRs have been characterized extensively because of their pharmacological relevance and ease of heterologous expression. The promise is that the wealth of functional information about well-studied GPCRs such as β2AR (Kobilka, 2013; Lefkowitz, 2013) may then be applied to examine OR functions in OSNs, including their functions in OR gene choice and OSN axonal wiring.

We have shown that the mouse β2-adrenergic receptor (β2AR) can substitute for a mouse OR in several ways (Feinstein et al., 2004). Puzzlingly, another group subsequently reported that *β2AR* is expressed endogenously in the main olfactory epithelium (MOE) (Hague et al., 2004), raising the question as to why β2AR expressed from the *M71* locus results in axonal coalescence into novel and distinct glomeruli. Transgenic β2AR expression driven by the *MOR23* promoter (Vassalli et al., 2002) also produces distinct glomeruli (Aoki et al., 2013; Nakashima et al., 2013).

* Corresponding author at: Max Planck Institute of Biophysics, Max Planck Research Unit for Neurogenetics, Max-von-Laue-Strasse 3, D-60438 Frankfurt, Germany.
E-mail address: peter.mombaerts@biophys.mpg.de (P. Mombaerts).

1044-7431/$ – see front matter © 2013 Elsevier Inc. All rights reserved.
http://dx.doi.org/10.1016/j.mcn.2013.10.010

Here, we have generated a novel gene-targeted strain in which mouse β2AR is expressed together with tauGFP from the *M71* locus. In mice of a cross of the two differentially tagged β2AR→M71 alleles, OSNs express either taulacZ or tauGFP but not both, thereby excluding an essential and specific role of the OR coding sequence in monoallelic expression (Nguyen et al., 2007). Patch-clamp recordings reveal that GFP+ OSNs respond to the β2AR agonist isoproterenol in a dose-dependent manner. Despite extensive analyses of β2AR gene and protein expression, we are not able to confirm the *β2AR* expression findings of Hague et al., 2004. Specifically, we do not find evidence of endogenous β2AR expression in M71+ OSNs. Moreover, β2AR and β1AR knockout mice have no overt defects in their olfactory system. Nonetheless, with the same in situ hybridization technique we can show that another GPCR gene, the dopamine type-2 receptor (*Drd2*), is strongly expressed in the MOE across all mature OSNs. Our results corroborate the experimental value of β2AR as a surrogate OR for studying various aspects of OR gene choice and axonal wiring.

Results

The β2AR→M71-IRES-tauGFP strain

We have generated and characterized a mouse strain carrying a β2AR→M71-IRES-taulacZ gene-targeted mutation (Feinstein et al., 2004), abbreviated β2AR→M71-lacZ (Fig. 1A). The design of this coding region replacement is such that OSNs that choose the mutant *M71* locus for expression do not produce M71 protein but β2AR instead. In order to enable physiological analysis of β2AR→M71 OSNs, we have now generated another mouse strain with a β2AR→M71-IRES-tauGFP gene-targeted mutation, abbreviated β2AR→M71-GFP (Fig. 1A). The design matches that of the β2AR→M71-IRES-taulacZ mutation, except for expression of the marker GFP instead of β-galactosidase.

The cell bodies of β2AR→M71-GFP OSNs are scattered within the dorsal MOE (Fig. 1B), as is the case for OSNs expressing M71 (Bozza et al., 2002) or β2AR→M71-lacZ (Feinstein et al., 2004). These OSNs display a dendritic knob from which cilia emanate (inset in Fig. 1B). The number of GFP+ cells in β2AR→M71-GFP homozygous mice aged three weeks is 1262 ± 132 (n = 3) per mouse. In situ hybridization (ISH) of the MOE shows that β2AR→M71-GFP OSNs are either *Omp*+ *Gap43*− (mature), *Omp*− *Gap43*+ (immature), or *Omp*+ *Gap43*+ (intermediate) (Fig. 1C). Quantification of the three stages reveals that, as a population, β2AR→M71-GFP OSNs are somewhat less mature compared to M71 OSNs (Fig. 1C). In a cross of β2AR→M71-GFP × β2AR→M71-lacZ mice, immunohistochemistry (IHC) for β-galactosidase combined with the intrinsic fluorescence of GFP shows that individual OSNs express either marker but not both (Fig. 1D1); we counted 636 GFP+ cells and 1162 lacZ+ cells, but no lacZ/GFP double-positive cells. Likewise, in a cross of β2AR→M71-lacZ × M71-IRES-tauGFP mice, OSNs express either marker but not both (Fig. 1D2); we counted 442 lacZ+ cells and 460 GFP+ cells, but no lacZ/GFP double-positive cells. Thus, the β2AR→M71-GFP allele is expressed monoallelically: with regard to the differentially tagged β2AR→M71-lacZ allele, and with regard to the tagged *M71* allele.

Do β2AR→M71-GFP OSNs coexpress an OR gene? Does the β2AR→M71-GFP mutant allele also follow the rule of monogenic expression? We addressed this difficult question by two- and three-color ISH, using riboprobes for *β2AR* and mixtures of *class I OR* genes (*mix 1* and *mix 2*) or *class II OR* genes (*mix 1* and *mix 2*). In three-color ISH (Fig. 1E1), cell bodies of OSNs react with either *class I mix 1* riboprobes, *class II mix 1* riboprobes, or with the *β2AR* riboprobe. In two-color ISH, we counted 28,324 OSNs reacting with *class I mix 1* (recognizing 6 OR genes) and 398 with *β2AR*; and 21,161 OSNs reacting with *class I mix 2* (recognizing 5 OR genes) and 437 with *β2AR*. Likewise, we counted 19,858 OSNs reacting with *class II mix 1* (recognizing 5 OR genes) and 398 with *β2AR*; and 17,774 OSNs reacting with *class II mix 2* (recognizing 12 OR genes) and 414 with *β2AR*. These staining patterns are consistent with monogenic expression of the β2AR→M71-GFP mutation; they strongly suggest that no OR gene is coexpressed.

Thus, our histological MOE studies demonstrate that the β2AR→M71-GFP allele behaves as a typical OR allele.

β2AR immunoreactivity is concentrated in the dendritic cilia of OSNs

Another characteristic of ORs is that OR proteins are concentrated in the chemoreceptive end of OSNs: the cilia that emanate from the dendritic knob (Barnea et al., 2004; Feinstein et al., 2004; Strotmann et al., 2004). We performed wholemount IHC of the MOE with antibodies against β2AR in β2AR→M71-GFP mice (Fig. 2A–D). In side views (Fig. 2A, B), β2AR immunoreactivity is strong in the dendrite, dendritic knob, and cilia of OSNs that express β2AR→M71-GFP. *En face* views (Fig. 2C, D) reveal strong β2AR immunoreactivity along the dozen or so dendritic cilia. In M71::GFP mice, which express a C-terminal fusion of GFP to M71 as a result of a gene-targeted mutation (Feinstein et al., 2004), there is a similar pattern of ciliary labeling in an *en face* view (Fig. 2E). Thus, expression of β2AR from the *M71* locus results in a concentrated β2AR immunoreactivity in the dendritic cilia of OSNs.

Coexpression of Gnal with β2AR

The β2AR normally stimulates G-protein pathways via G_{α}s, the protein product of the *Gnas* gene. Mature OSNs express G_{α}olf (Jones and Reed, 1989), the protein product of the *Gnal* gene. G_{α}olf is an essential component of the odorant-evoked signal transduction pathway (Belluscio et al., 1998), and β2AR can also signal via G_{α}olf (Liu et al., 2001). In the MOE of wild-type C57BL/6 mice aged three weeks, three-color ISH reveals expression of *Gnal* throughout the thickness of the MOE except basally, and largely together with *Omp* (Fig. 3A). By contrast, *Gnas* is expressed strongly in the basal MOE, below the

Fig. 1. The β2AR→M71-IRES-tauGFP mouse strain.(A) Generation of the β2AR→M71-IRES-tauGFP strain by gene targeting, abbreviated β2AR→M71-GFP. The *M71* coding sequence, which consists of one exon, is replaced with the coding sequence of mouse *β2AR*. The *IRES-tauGFP-ANCF* cassette is inserted three nucleotides after stop codon of *β2AR* by homologous recombination in ES cells. The *ACNF* cassette, a self-excising *neo* gene, has been removed during transmission though the male germ line, leaving a single *loxP* site (red triangle) behind in the locus. The β2AR→M71-IRES-taulacZ targeted mutation (Feinstein et al., 2004) is shown for comparison, and abbreviated β2AR→M71-lacZ.(B) Medial wholemount view of the MOE and turbinates of a β2AR→M71-GFP mouse. The inset shows GFP+ cells at high magnification.(C) (Left) Three-color ISH of the MOE of a β2AR→M71-GFP mouse with riboprobes for *Gap43* (immature OSNs), *Omp* (mature OSNs), and *β2AR*. Examples are shown of a *β2AR*+ cell that is *Omp*+ *Gap43*− (left panel), *Omp*− *Gap43*+ (middle panel), or *Omp*+ *Gap43*+. (Right) Quantification of the percentages of *M71*+ or *β2AR*+ cells that are mature (*Omp*+), immature (*Gap43*+), or at an intermediate stage of maturity (*Omp*+ *Gap43*+). Three-color ISH was performed on the MOE of β2AR→M71-GFP × M71-RFP mice aged three weeks with *Omp*, *Gap43*, and *β2AR* or *RFP* (for *M71*) riboprobes. The population of *β2AR*+ cells is less mature than the population of *M71-RFP*+ cells, within the same mouse. For each genotype four mice were analyzed. Single asterisk shows significance <0.05 by Student's *t*-test.(D) Monoallelic expression of the β2AR→M71 targeted mutations. IHC of the MOE of a β2AR→M71-GFP × β2AR→M71-lacZ mouse (D1), and a M71-GFP × β2AR→M71-lacZ mouse (D2). Sections were stained with anti-β-galactosidase antibodies followed by Alexa 546-conjugated secondary antibodies. The GFP signal is from its intrinsic fluorescence. Individual OSNs are either red-fluorescent or green-fluorescent, but not both.(E) Monogenic expression of the β2AR→M71-GFP targeted mutation. E1, Three-color ISH of the MOE of a β2AR→M71-GFP mouse with *class I mix 1* and *class II mix 1* riboprobes. Cells are labeled in only one color. E2, Two-color ISH of the MOE of a β2AR→M71-GFP mouse with riboprobes for *β2AR* and *class I mix 1*. Cells are either labeled red or green but not both. E3, Two-color ISH of the MOE of β2AR→M71-GFP mice with riboprobes for *β2AR* and *class II mix 2*. Cells are either labeled red or green but not both.Scale bars, 200 μm in B; 20 μm in inset of B; 10 μm in C, D1, D2, E2, E3; 50 μm in E1.

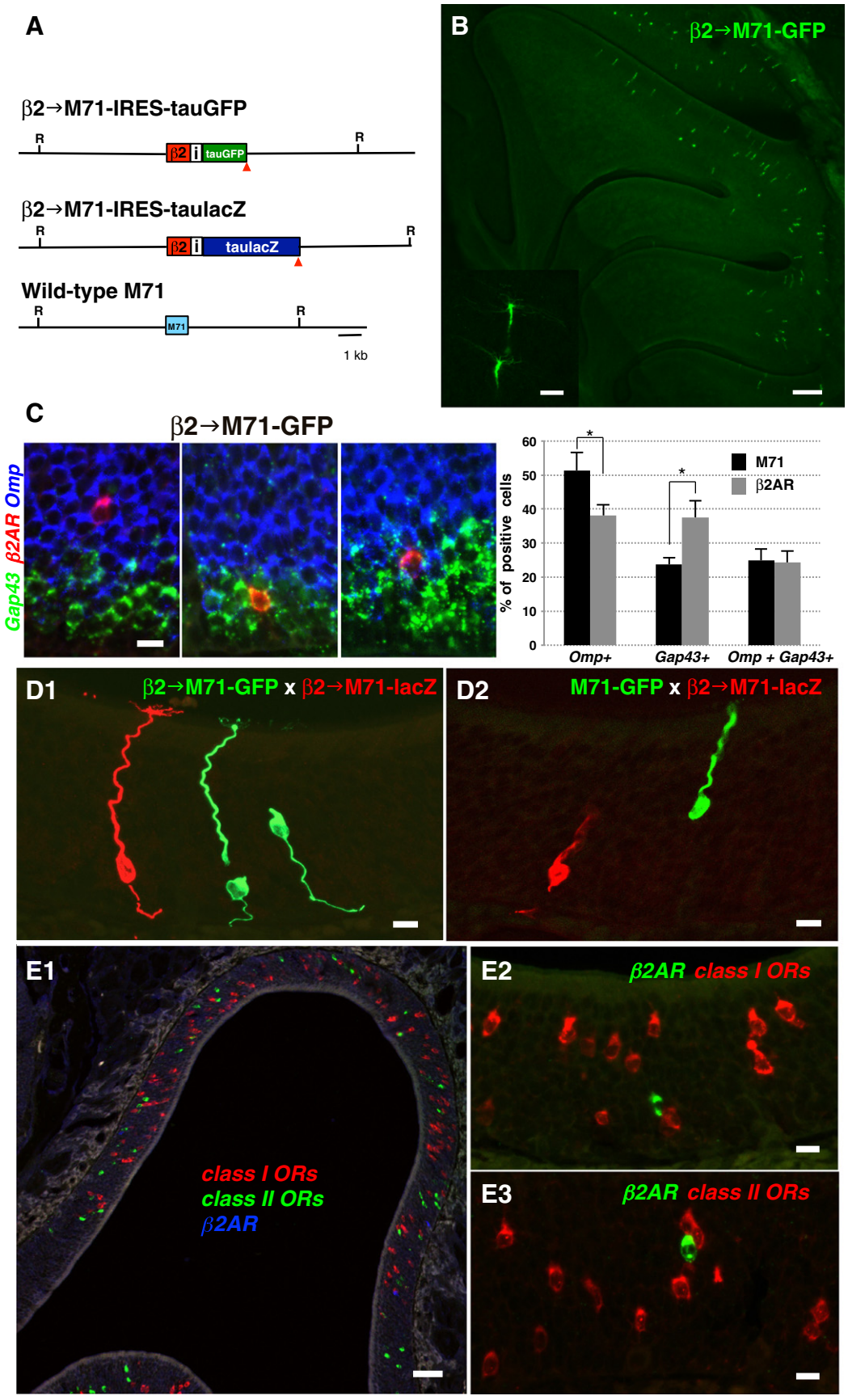
A
β2→M71-IRES-tauGFP
R
β2
i
tauGFP
R
β2→M71-IRES-taulacZ
R
β2
i
taulacZ
R
Wild-type M71
R
M71
R
1 kb
B
β2→M71-GFP
C
β2→M71-GFP
Gap43 β2AR Omp
% of positive cells
60
50
40
30
20
10
0
M71
β2AR
Omp+
Gap43+
Omp + Gap43+
D1
β2→M71-GFP x β2→M71-lacZ
D2
M71-GFP x β2→M71-lacZ
E1
class I ORs
class II ORs
β2AR
E2
β2AR class I ORs
E3
β2AR class II ORs

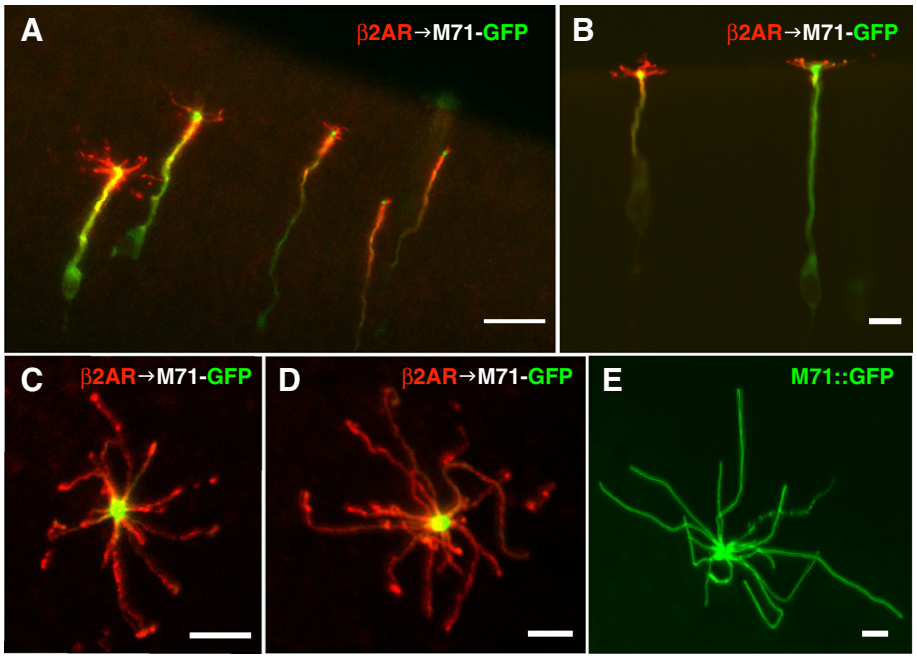

Fig. 2. Concentrated subcellular localization of β2AR protein in the cilia of β2AR→M71-GFP OSNs. (A–B) Wholemount IHC of the MOE of a β2AR→M71-IRES-tauGFP mouse stained with antibodies against β2AR. The GFP signal is from its intrinsic fluorescence. In these side views, β2AR proteins are located in the cilia of GFP+ OSNs but not in other OSNs. (C–D) Wholemount IHC of the MOE of a β2AR→M71-IRES-tauGFP mouse stained with antibodies against β2AR. The GFP signal is from its intrinsic fluorescence. In these *en face* views, β2AR proteins are located in the cilia of GFP+ OSNs but not in the adjacent OSNs. The tauGFP axonal marker labels the cilia less intensely than antibodies against β2AR. Strong colocalization occurs in the dendritic knob, which appears yellow in these merged images. (E) Wholemount *en face* view of the cilia of GFP+ OSN of a M71::GFP mouse, in which GFP is fused by gene targeting to the C-terminus of the M71 (Feinstein et al., 2004). The GFP signal is from its intrinsic fluorescence. The M71::GFP fusion protein is distributed along the cilia, comparable to β2AR protein in C–D. Scale bars, 20 μm in A; 10 μm in B; 5 μm in C–E.

layer of *Gap43*+ cells (Fig. 3B), and mutually exclusively with *Gnal* (Fig. 3C). There are also apical *Gnas* signals, in sustentacular cells. In β2AR→M71-GFP mice, cell bodies of GFP-immunoreactive OSNs coexpress *Gnal* and rarely *Gnas* (Fig. 3C). Thus, based on *Gnal* and *Gnas* expression, β2AR+ OSNs have the potential to transduce responses evoked by β2AR agonists such as isoproterenol.

β2AR→M71-GFP neurons respond to isoproterenol

We next performed patch-clamp recordings on the dendritic knobs of β2AR→M71-GFP OSNs with isoproterenol, using a well-characterized intact *ex vivo* preparation (Grosmaitre et al., 2006, 2007, 2009; Lam and Mombaerts, 2013; Lee et al., 2011; Ma et al., 1999). In voltage-clamp mode, seven out of seven β2AR→M71-GFP OSNs responded to a 10^{-4} M stimulus of isoproterenol with inward currents (Fig. 4A). Five cells were exposed to 10^{-4} M of acetophenone, a stimulus for M71+ OSNs (Bozza et al., 2002); none responded. IBMX and forskolin, general activators of the signal transduction pathway, resulted in inward currents in all seven recorded OSNs (Fig. 4A). Increasing concentrations of isoproterenol, ranging from 10^{-7} to 10^{-3} M, induced inward currents with increasing maximum amplitude. We recorded dose–response curves from three β2AR→M71-GFP OSNs (Fig. 4B). The peak transduction currents versus the concentration were plotted and fitted with the Hill equation: $I = Imax / (1 + (K_{1/2} / C)^n)$, where I represents the peak current, Imax the maximum response at saturating concentrations, $K_{1/2}$ the concentration at which half of the maximum response was reached, C the concentration of odorant and n the Hill coefficient. The average maximum amplitude elicited by saturating concentrations is 109.9 ± 6.6 pA; the $K_{1/2}$ is 8.37 ± 2 μM, and the Hill coefficient is 0.71 ± 0.16. By contrast, in 12 out of 12 randomly chosen OSNs of wild-type C57BL/6 mice, no responses to isoproterenol were observed at 10^{-5} to 10^{-4} M (Fig. 4C). Expression of an endogenous, unknown OR gene in these OSNs is indicated by responses to an odorant mixture in 8 of these 12 OSNs (Fig. 4C). Thus, expression of β2AR from the *M71* locus in OSNs confers a dose-dependent responsiveness to isoproterenol, but such responses are not detected in wild-type OSNs.

Coalescence of axons from β2AR→M71-GFP OSNs into glomeruli

A hallmark of mouse OSNs that express the same OR gene is that their axons coalesce into one or a few homogeneous glomeruli in the medial and lateral halves of the OB, at conserved positions. Axonal coalescence can be demonstrated readily by IRES-mediated cotranslation of an axonal marker such as taulacZ (Mombaerts et al., 1996) or tauGFP (Rodriguez et al., 1999). We have previously shown that axons from β2AR→M71-lacZ OSNs coalesce into homogeneous glomeruli that are distinct and remote from the endogenous M71 glomeruli (Feinstein et al., 2004). We now confirm and extend this observation for axons from β2AR→M71-GFP OSNs (Fig. 5A). The β2AR→M71 glomeruli are smaller than the M71 glomeruli, but they are discrete and apparently homogeneous glomeruli. At two weeks, the number and diameter of glomeruli in β2AR→M71-GFP mice are 2.3 ± 0.3 (SEM, n = 13 bulbs, 46% of bulbs have two glomeruli) and 20.0 μm ± 1.26 (n = 35 bulbs), compared to 2.1 ± 0.1 (n = 9 bulbs, 89% of bulbs have two glomeruli) and 44.1 μm ± 1.28 (n = 19) in M71-IRES-tauGFP mice; there is a significant difference in the glomerular diameter between β2AR→M71-GFP mice and M71-IRES-tauGFP mice (*t*-test, p = 4.309E−17) but not in the number (p = 0.6314). The smaller glomerular diameter in β2AR→M71-GFP mice correlates with the smaller number of GFP+ OSNs. Although there is more variance in the number of glomeruli in β2AR→M71-GFP mice, there is no significant difference in this number between β2AR→M71-GFP mice and M71-IRES-tauGFP mice (Fisher's exact test, p = 0.074). At three weeks, the number and diameter of glomeruli in β2AR→M71-GFP mice are 2.1 ± 0.3 (n = 9) and 17.8 μm ± 1.26 (n = 22); there is no significant difference between two and three weeks (Fisher's exact test, number p = 0.999; *t*-test,

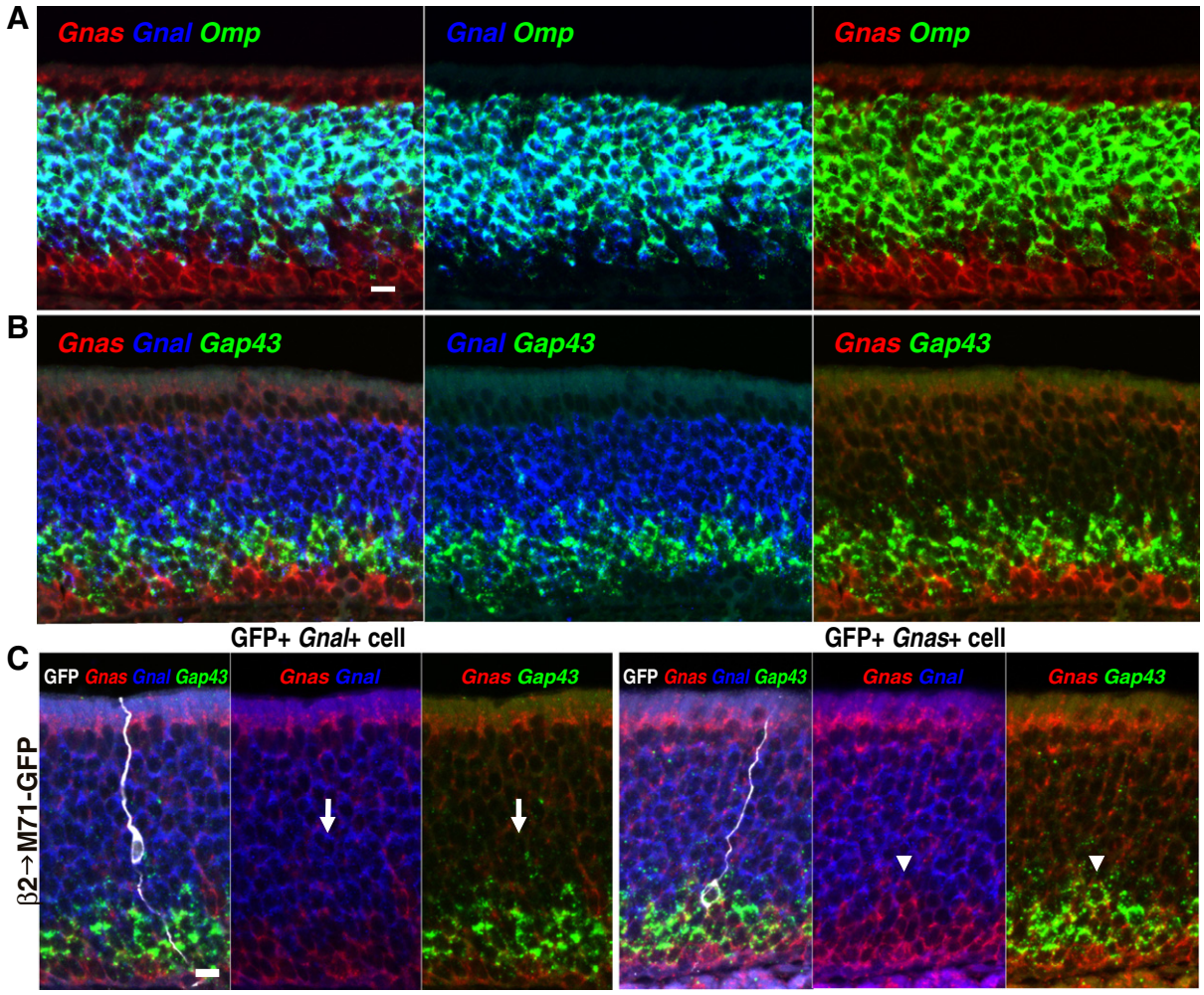

Fig. 3. In situ hybridization of the MOE with *Gnas* and *Gnal*. (A) Three-color ISH of the MOE with riboprobes for *Gnas*, *Gnal*, and *Omp*, in a C57BL/6 mouse aged three weeks. *Gnal* is expressed in *Omp*+ cells. *Gnas* and *Omp* are not co-localized. Sustentacular cells (apical) express *Gnas*. (B) Three-color ISH of the MOE with riboprobes for *Gnas*, *Gnal*, and *Gap43*, same mouse as in A. *Gnas* expression is more basal than *Gap43* expression. Some of the basal *Gap43*+ cells coexpress *Gnas*. (C) Three-color ISH combined with single-color IHC of the MOE with riboprobes for *Gnas*, *Gnal* and *Gap43*, and anti-GFP antibody, in a homozygous β2AR→M71-GFP mouse aged three weeks. (Left panels) GFP+ cell coexpressing *Gnal*, cell body indicated with arrow. (Right panels) A rare GFP+ cell coexpressing *Gnas* and *Gap43*, cell body indicated with arrowhead. Scale bar in A, 10 μm.

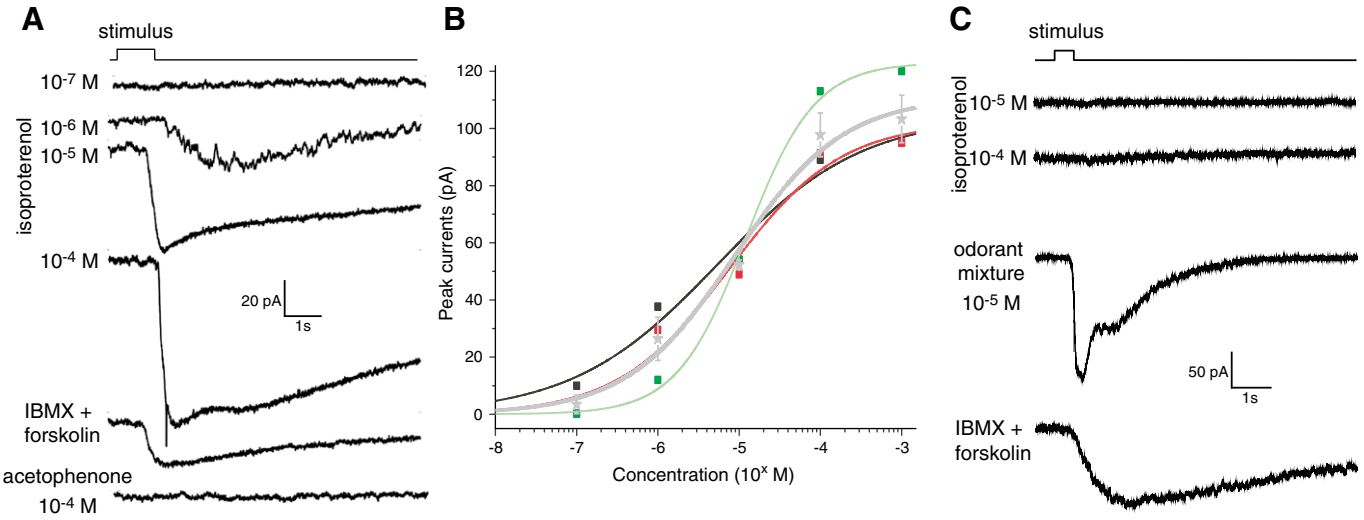

Fig. 4. β2AR→M71-GFP but not wild-type OSNs respond to the β2AR agonist isoproterenol. (A) Representative traces of isoproterenol-induced inward currents in an individual β2AR→M71-GFP cell from a homozygous mouse. The cell also responded to IBMX and forskolin, but not to the M71 ligand acetophenone. The holding potential was −60 mV. (B) Dose–response curve of β2AR→M71-GFP cells. Curves for three individual cells are in green, red, and black; the curve for the averages is in gray. (C) A randomly chosen OSN from a non-genetically modified C57BL/6 mouse did not respond to isoproterenol, but did respond to IBMX + forskolin, and to the odorant mixture.

diameter p = 0.244). The distance between β2AR→M71 glomeruli and M71 glomeruli in the medial half of the olfactory bulb (Fig. 5B) is quite large: 949 ± 277 μm (n = 16). In a β2AR→M71-GFP × β2AR→M71-lacZ cross, the two types of axons coalesce into the same glomeruli, where they comingle diffusely without any signs of segregation (Fig. 5C1,C2,C4). The β2AR→M71 glomeruli also show strong β2AR immunoreactivity (Fig. 5C3). Thus, based on the fundamental principle of axonal coalescence into glomeruli, expression of β2AR from the *M71* locus is indistinguishable from expression of an OR from an *OR* locus.

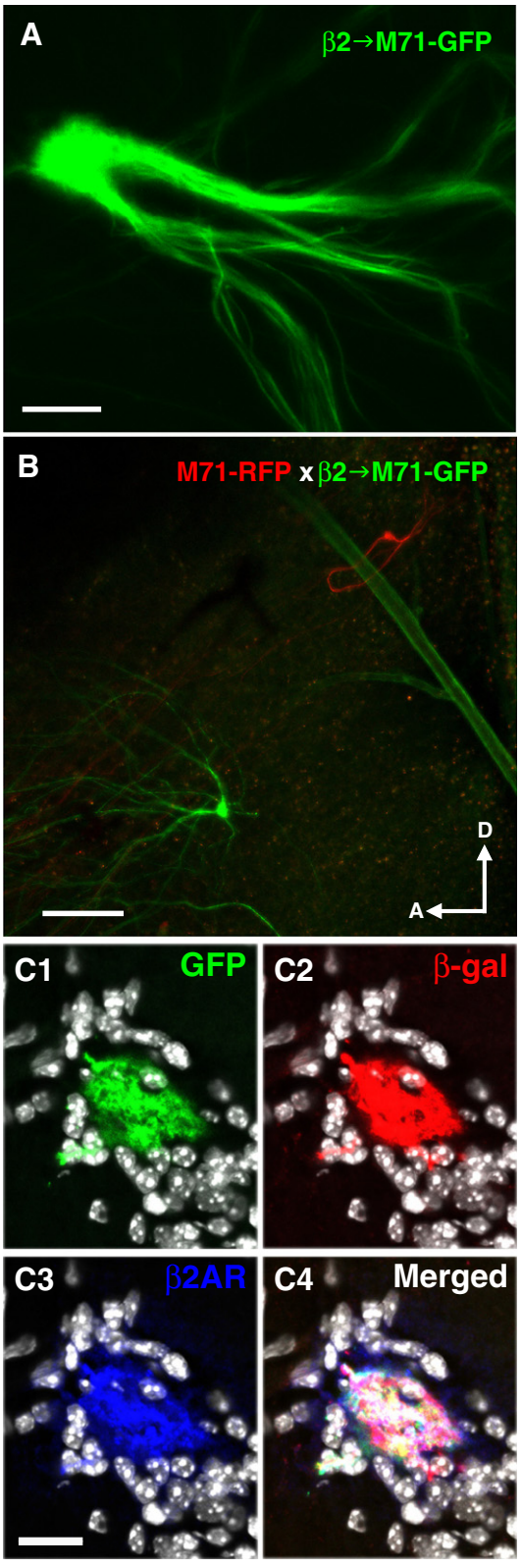

The MOE and olfactory bulb of β2AR and β1AR knockout mice

There has been one report about endogenous β2AR expression in the mouse MOE, by radioactive ISH (Hague et al., 2004). We have not been able to confirm expression in OSNs of the MOE, by fluorescent ISH and by IHC. By strongly increasing the gain of the imaging, a faint and diffuse fluorescent signal can be seen with antibodies against β2AR in the MOE of wild-type mice (Fig. 6A). But this signal is also seen in β2AR knockout mice (Chruscinski et al., 1999) (β2AR-KO) (Fig. 6A), indicating that it is background. In GFP + OSNs of M71-IRES-tauGFP mice, we do not detect β2AR immunoreactivity either, whereas β2AR signal is clear and intense in β2AR→M71-GFP OSNs (Fig. 6A).

Despite any signs of expression of β2AR and β1AR in OSNs, we proceeded to examine the MOE of β2AR-KO mice and of β1AR-KO mice (Rohrer et al., 1996). We find a normal layering of *Gap43* + cells (immature OSNs), *Omp* + cells (mature OSNs), and *Cbr2* + cells (sustentacular cells) in three-color ISH (Fig. 6B). Moreover, two hallmarks of an OR, the concentration of OR protein in dendritic cilia and axonal coalescence into glomeruli, are not affected in β2AR-KO mice and β1AR-KO mice crossed with M71::GFP mice (Fig. 6C). Finally, tyrosine hydroxylase immunoreactivity, an activity marker for periglomerular neurons in the olfactory bulb, is not affected in β2AR-KO mice and β1AR-KO mice (Fig. 6D). As expected, this immunoreactivity is essentially absent in Cnga2 knockout mice, in which the odorant-evoked signal transduction pathway is impaired (Fig. 6D).

However, using the same fluorescent ISH technique, we do find widespread and strong expression of another GPCR in the MOE, and across mature OSNs: the dopamine type-2 receptor, *Drd2* (Fig. 7). Thus, with the same ISH method and in the same hands, *Drd2* expression is readily detectable in OSNs, but *β2AR* expression is not detectable.

Discussion

The β2AR as a surrogate odorant receptor

We have shown previously that β2AR expression from the *M71* locus along with IRES-taulacZ (β2AR→M71-lacZ) is in several aspects phenotypically indistinguishable from expression of an OR coding sequence from the *M71* locus (Feinstein et al., 2004). We have here confirmed and extended these findings in a novel strain of β2AR→M71-GFP mice. The important advantage of the GFP marker is that it lends itself well to electrophysiological recordings. The GFP + cells express *Gnal* and respond to the β2AR agonist isoproterenol in a dose-dependent manner with $K_{1/2}$ of 8.37 μM, which is similar to the 10 μM concentration used for other studies in the mouse olfactory system (Araneda and Firestein, 2006). Thus, by the criterion of "odorant" responses, we have here demonstrated a critical function of β2AR as a surrogate OR in OSNs: it confers dose-dependent responsiveness to a cognate agonist. We also demonstrate strong β2AR immunoreactivity in OSN cilia. Function of β2AR as a surrogate OR in OSNs under these experimental conditions is consistent with motifs in intracellular regions 2, 3, and 4 that are

Fig. 5. Glomeruli formed by coalescence of axons of β2AR→M71-GFP OSNs. (A) Medial wholemount view of the olfactory bulb of a β2AR→M71-GFP mouse aged three weeks. Axons labeled with intrinsic GFP fluorescence coalesce into a single medial glomerulus. (B) Medial wholemount view of the olfactory bulb of a M71-RFP × β2AR→M71-GFP mouse. Axons and glomeruli are labeled by the intrinsic fluorescence of RFP and GFP. The medial β2AR→M71-GFP glomerulus is shifted anteriorly and ventrally compared to the endogenous M71-RFP glomerulus. Both glomeruli are small, as they receive axonal input from half of the OSNs that express the *M71* locus. (C) IHC of a section of the olfactory bulb of a β2AR→M71-GFP × β2AR→M71-lacZ mouse, stained with antibodies against β-galactosidase and β2AR. The GFP signal is from its intrinsic fluorescence, and the white signal is from DAPI. Axons of GFP + OSNs coalesce and comingle with axons from lacZ + OSNs within a single lateral glomerulus. Scale bars, 20 μm in A and C3; 200 μm in B.

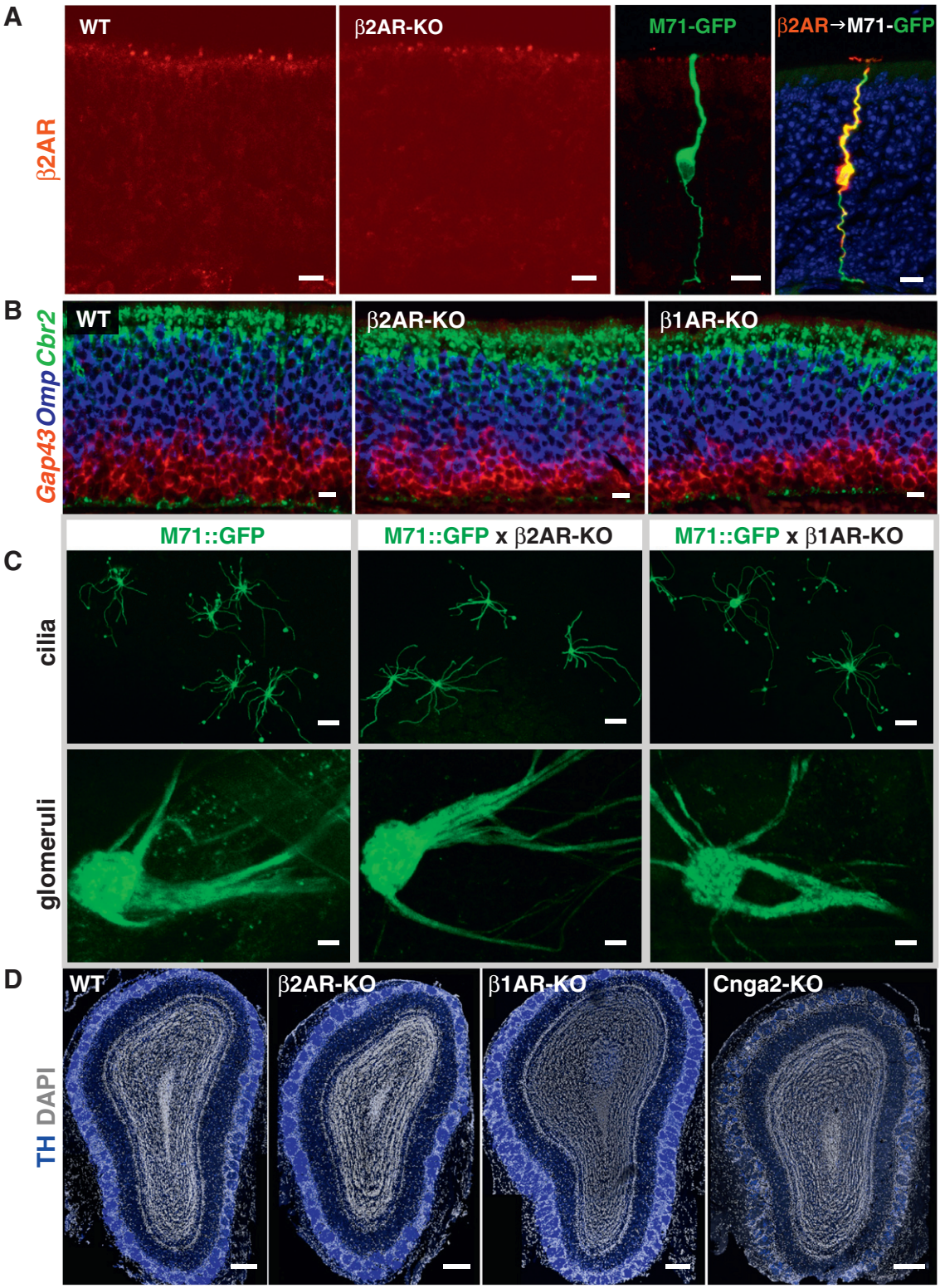

Fig. 6. The olfactory system of β2AR and β1AR knockout mice. (A) IHC of the MOE of wild-type, β2AR-KO, M71-GFP, and β2AR→M71-GFP mice with antibodies against β2AR conjugated with Alexa 546 (red). The GFP signal is from its intrinsic fluorescence. DAPI counterstains nuclei in blue, in the right-most panel. There is no β2AR signal in WT, β2AR-KO, and M71-GFP mice, even when the gain is increased considerably. A strong β2AR signal is seen in the cell body, dendrite, and cilia of the β2AR→M71-GFP cell. (B) Three-color ISH with *Cbr2*, *Omp*, and *Gap43* riboprobes. The MOE of the wild-type mouse shows the three layers of sustentacular cells (apical, *Cbr2*+), mature neurons (middle, *Omp*+), and immature neurons (basal *Gap43*+). This three-layered structure is preserved in the MOE of β2AR-KO and β1AR-KO mice. (C) Subcellular localization of M71::GFP fusion proteins in OSN cilia and glomeruli. The GFP signal is from its intrinsic fluorescence. The intensity and patterns of the GFP signal in cilia (upper panels) and glomeruli (lower panels) in M71::GFP × β2AR-KO and M71::GFP × β1AR-KO double mutant mice are indistinguishable from those in M71::GFP mutant mice. (D) IHC of coronal sections of the olfactory bulb of wild-type (WT), β2AR-KO, β1AR-KO, and Cnga2-KO mice, with antibodies against tyrosine hydroxylase (TH), an activity marker in periglomerular neurons. Staining patterns are indistinguishable in WT, β2AR-KO, and β1AR-KO mice; there is no staining in the hemizygous Cnga2-KO male, reflecting the overwhelming lack of odorant-evoked signaling in its OSNs. Scale bar, 10 μm in A, B and C—cilia; 20 μm in C—glomeruli; and 200 μm in D.

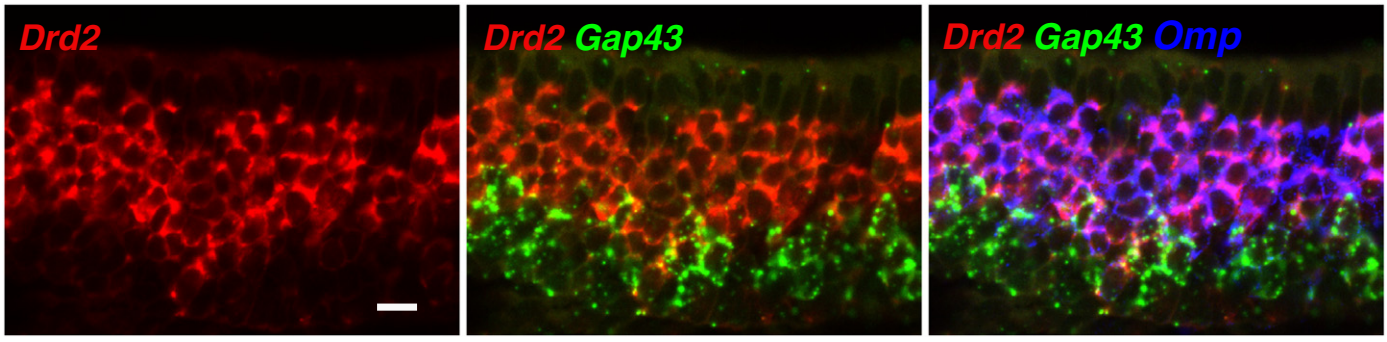

Fig. 7. *Drd2* expression in mature OSNs. Three-color ISH of the MOE with *Drd2*, *Omp*, and *Gap43*. Mature OSNs express *Drd2*. Scale bar, 10 μm.

conserved among ORs and other GPCRs (DRYVAI, KAL, and NPXIY, respectively), and with coupling of β2AR to G_{α}olf (Jones and Reed, 1989; Liu et al., 2001).

Our results with differentially tagged β2AR→M71 alleles provide powerful evidence that the OR coding sequence does not fulfill a specific role in monoallelic expression of an OR locus (Nguyen et al., 2007); its role can be substituted by β2AR. The principle of monogenic expression of β2AR (one OR gene per OSN) is more difficult to demonstrate convincingly. The β2AR→M71 axons innervate their glomeruli exclusively and homogeneously, suggesting that these glomeruli do not receive axonal innervation from OSNs that express other ORs. Here are two arguments for monogenic expression. If any of several other ORs were to be coexpressed with β2AR→M71, labeled axons would likely innervate a variety of glomeruli, appropriate for these coexpressed ORs. It is difficult to imagine a mechanism that governs the coexpression of a specific OR with β2AR→M71, but it cannot be excluded. We have addressed the issue of monogenic expression of β2AR→M71 by ISH with riboprobes for *β2AR* and mixtures of class I and class II OR genes: we do not observe coexpression in a total of 1647 *β2AR*+ cells and a total of 87,117 cells labeled with the OR riboprobes. As there is no indication for OR expression in β2AR→M71 OSNs, single-cell RT-PCR experiments with degenerate primers for OR genes are likely to yield only artifacts.

Our new findings and those of others (Aoki et al., 2013; Nakashima et al., 2013) corroborate the experimental value of β2AR as a surrogate OR. The implication and promise are that the wealth of pharmacological knowledge about structure–function relationships of β2AR can be applied to study aspects of OR function in OSNs.

Endogenous β2AR expression in OSNs

The use of β2AR as a surrogate OR is predicated on the absence of endogenous β2AR expression in OSNs. There has been a single report of β2AR expression in the MOE, which was based on radioactive ISH (Hague et al., 2004). Despite major attempts to visualize β2AR gene and protein expression histologically in OSNs, we have not been able to confirm this finding. Randomly chosen OSNs from non-genetically modified, wild-type C57BL/6 mice do not respond to the β2AR agonist isoproterenol at 10^{-5} to 10^{-4} M. Further, the MOE of β2AR knockout mice and β1AR knockout mice appears normal. We cannot exclude expression of β2AR in a small subpopulation of OSNs, or in non-OSN cell types of the MOE. Due to low cellular resolution, the ISH method used by Hague et al. (2004) does not afford the conclusion that β2AR is expressed in mature OSNs. We cannot exclude low-level expression of β2AR in some or many OSNs, below the detection threshold of our ISH and IHC methods. Sensitive methods such as radioactive ISH, qPCR, or NanoString (Khan et al., 2011; 2013) may reveal trace amounts of β2AR in the MOE or in OSNs. In any case, as β2AR has been proposed to "drive" OR surface expression (Bush and Hall, 2008; Bush et al., 2007; Hague et al., 2004), expression in OSNs ought to be strong, perhaps stoichiometric with ORs. The increase in M71 surface expression in human embryonic kidney-293 cells by coexpression with β2AR (Hague et al., 2004) may be an example of the caveats of heterologous (over)expression, and have limited *in vivo* relevance. Effects of adrenaline on OSNs have been documented in the newt (Kawai et al., 1999).

Expression of non-olfactory GPCRs in OSNs

Regardless of the controversy about endogenous β2AR expression in OSNs, there are several independent lines of evidence for expression of non-olfactory GPCRs in OSNs. This expression is of particular interest if it involves functional interactions with ORs such as by heterodimerization or oligomerization. M71-expressing OSNs in gene-targeted M71-IRES-taulacZ mice (Feinstein and Mombaerts, 2004) show immunoreactivity for purinergic receptors $P2Y_1R$, $P2Y_2R$, and $A_{2A}R$ (Bush et al., 2007; Bush and Hall, 2008). The M3 muscarinic acetylcholine receptor, product of the *Chrm3* gene, is expressed in the MOE, and increases the potency and efficacy of odorant-elicited responses of several ORs in human embryonic kidney-293T cells (Li and Matsunami, 2011). *Drd2* expression in OSNs has been documented histologically in rat (Koster et al., 1999) and mouse (Sammeta et al., 2007), and electrophysiologically in rat (Ennis et al., 2001; Okada et al., 2003) and mouse (Hegg and Lucero, 2004). We confirm with fluorescent ISH that *Drd2* is expressed strongly and uniformly across mature OSNs in mouse. Thus, with the same ISH method and in the same hands, we can readily detect *Drd2* expression in OSNs, but not *β2AR* expression. There is chromogenic ISH evidence for several other non-olfactory GPCRs in mouse OSNs (Sammeta et al., 2007).

Even if these non-olfactory GPCRs do not interact directly with ORs, their signaling pathways may overlap – for instance they may couple to the same G protein subunits as ORs: to G_{α}s or G_{α}olf – and they may also have agonist-independent activity, in addition to that of ORs (Nakashima et al., 2013). Expression of non-olfactory GPCRs in OSNs must be taken into account when formulating hypotheses about OR gene choice and OSN axonal wiring that do not assign unique functions to ORs, particularly when these non-olfactory GPCRs are expressed at stages of OSN differentiation when these processes take place.

Experimental methods

Gene targeting

We mutated the *M71* locus by homologous recombination in ES cells according to the same design as for numerous other targeted *M71* alleles (Feinstein et al., 2004). We replaced the *M71* coding sequence with the mouse *β2AR* coding sequence and the *IRES-tauGFP-ANCF* cassette (Bozza et al., 2002), which we inserted three nucleotides after the stop codon of *β2AR*. The *ACNF* cassette, a self-excising *neo* gene, is removed during transmission though the male germ line, leaving a single *loxP* site behind. The targeting vector was linearized and electroporated into E14 embryonic stem (ES) cells according to standard methods (Mombaerts et al., 1996). ES cells were injected into C57BL/6 blastocysts, and chimeras bred with wild-type C57BL/6 mice.

Using genomic DNA of mouse tails, we confirmed that the sequence of *β2AR* at the *M71* locus encodes the wild-type mouse *β2AR* amino acid sequence. The strain is in a mixed 129 × C57BL/6 background, and publicly available from The Jackson Laboratory (Bar Harbor, ME) as JR#6734, official strain name B6;129P2-Olfr151 < tm35(Adrb2) Mom > /MomJ. Both males and females were used for experiments.

In situ hybridization and X-gal staining

Multicolor in situ hybridization (ISH) and ISH combined with IHC were performed as described (Ishii et al., 2004). To identify mature, immature, and intermediate stages of *β2AR*+ cells and *M71*+ cells, we analyzed by three-color ISH every tenth section of 12 μm coronal sections of the MOE (from the first appearance of the turbinates to the end of the MOE) from β2AR→M71 × M71-IRES-tauRFP mice aged three weeks (n = 4). Riboprobes were: *β2AR*, nt 208–1464 from GenBank accession number NM_007420; *Omp*, *Gap43* (Ishii et al., 2004); *RFP* (*mCherry*) as nt 21–512 from AY678264; and bovine *tau* (Ishii and Mombaerts, 2008), which was added to the *RFP* probe to enhance the signal of *tauRFP*. Images were collected with a Zeiss LSM 710 confocal microscope.

To address monogenic *β2AR* expression in β2AR→M71 mice, we analyzed β2AR→M71 mice aged three weeks (n = 3) with two- or three-color ISH. Riboprobes in *class I mix 1* are: *MOR7-1 (Olfr578)*, nt 382–869 from NM_147115.1; *MOR22-2 (Olfr69)*, nt 605–1117 from NM_013621.3; *MOR32-4 (Olfr672)*, nt 1–937 from NM_146760.1; *MOR40-1 (Olfr683)*, nt 1–960 from NM_147045.1. These riboprobes detect a total of six OR genes, including *Olfr68* and *Olfr684*. Riboprobes in *class I mix 2* are: *MOR18-2 (Olfr78)*, nt 1216–2164 from NM_130866.4; *MOR31-2 (Olfr690)*, nt 89–1022 from NM_020290.2; *MOR31-6 (Olfr691)*, nt 147061.1; *S50 (MOR42-1, Olfr545)*, nt 340–925 from NM_146840.1. These riboprobes detect a total of five OR genes, including *Olfr544*. Riboprobes in *class II mix 1* are: *MOR200-1 (Olfr1031)*, nt 347–867 from NM_001011759.2; *MOR258-5 (Olfr62)*, nt 167–883 from NM_146315.2; *MOR265-2P (Olfr819)*, nt 1–531 from NM_001165944.1; *MOR23 (MOR267-13,Olfr16)*, nt 49–940 from NM_008763.2. These riboprobes detect five OR genes, including *Olfr247*. Riboprobes in *class II mix 2* are: *MOR101-1* (*Olfr520*), nt 115–884 from NM_147063; *MOR126-1* (*Olfr54*), nt 1–942 from NM_010997.1; *MOR136-14* (*Olfr3*), nt 17–871 from NM_206903.1; *MOR259-13* (*Olfr1328*), nt 27–942 from NM_146399. These riboprobes detect a total of 12 OR genes, including *Olfr521*, *Olfr1329*, *Olfr1330*, *Olfr1331*, *Olfr1333*, *Olfr1335*, *Olfr1337*, and *Olfr1338*. The riboprobe for *Gnas* is nt 408–1512 from NM_001077510.2, *Gnal* is nt 1–1106 from NM_010307. For three-color ISH combined with IHC, chicken anti-GFP antibody (1:300, Abcam) followed by Alexa 647-conjugated goat anti-chicken IgG was used in β2AR→M71-GFP mice. The DNP-labeled *Gnal* riboprobe was detected by anti-DNP antibody (1:800, Invitrogen) followed by Alexa 405-conjugated goat anti-rabbit IgG (1:200, Invitrogen). The ISH riboprobe for *Drd2* is nt 524–1323 from NM_010077.2. The *Cbr2* probe is as in Ishii et al. (2004).

X-gal staining was done as described (Mombaerts et al., 1996) with minor modification: tissues were fixed in 4% paraformaldehyde (PFA) in 1× PBS without $MgSO_4$ and EGTA.

Immunohistochemistry on tissue sections

Mice were anesthetized by injection of ketamine HCl and xylazine (150 mg/kg and 10 mg/kg body weight, respectively), and perfused with ice-cold PBS, followed by 4% PFA in PBS. The mouse heads were dissected, post-fixed in 4% PFA, and decalcified in 0.45 M EDTA in 1× PBS overnight at 4 °C. The decalcification step was omitted for the bulbs. Samples were cryoprotected in 15% and 30% sucrose in 1× PBS at 4 °C, frozen in OTC compound, and sectioned at 12 or 16 μm with a Leica CM3500 cryostat. Sections were washed with 1× PBS and blocked with 10% NGS or NDS, 0.1% Triton X-100 in 1× PBS for 1 h at room temperature. After the blocking step, sections were incubated in 3% BSA, 0.1% Triton X-100 in 1× PBS overnight at 4 °C with rabbit anti-β-galactosidase (1:1000, Cappel, Fig. 1*D1*, *D2*), chicken anti-β-galactosidase (1:500, Abcam, Fig. 5*C2*), rabbit anti-β2AR (1:500, Santa Cruz, Figs. 5*C3*, 6*A*), and rabbit anti-TH (1:500, Millipore, Fig. 6*D*). The GFP signal is from its intrinsic fluorescence. After incubation with primary antibodies, sections were incubated for 2 h at room temperature with secondary antibodies: Alexa 546-conjugated goat anti-rabbit IgG (1:500, Invitrogen, Fig. 1*D1*, *D2*), Alexa 546-conjugated goat anti-chicken IgG (1:500, Invitrogen, Fig. 5*C2*), or Alexa 647-conjugated goat anti-rabbit IgG (1:500, Invitrogen, Fig. 5*C3*). The bulb sections were counterstained with 0.1 μg/ml DAPI (Invitrogen). Sections were analyzed with a Zeiss LSM 710 confocal microscope.

Wholemount immunohistochemistry

Wholemount IHC was performed as described (Strotmann et al., 2004). Briefly, olfactory turbinates and MOE were dissected from 2-wk or 3-wk old mice. Tissues were fixed in 4% PFA in 1× PBS for 4 h on ice, washed with 0.1% Triton X-100 in 1× PBS, and blocked with 10% NGS, 0.1% Triton X-100 in 1× PBS for 1 h at room temperature with gentle agitation. Incubation was at 4 °C overnight with gentle agitation in 1× PBS containing 10% NGS, 0.1% Triton X-100 with rabbit anti-β2AR (1:500, Santa Cruz). After washing with 0.1% Triton X-100 in 1× PBS, tissues were incubated with Alexa 546-conjugated goat anti-rabbit IgG (1:500, Invitrogen) in 1× PBS containing 10% NGS, 0.1% Triton X-100 for 2 h at room temperature. After washing with 0.1% Triton X-100 in 1× PBS, stained samples were kept in 1× PBS, and images of samples from *en face* views were collected with a Zeiss LSM 710 confocal microscope.

Patch-clamp recordings

Mice were anesthetized by injection of ketamine HCl and xylazine (150 mg/kg and 10 mg/kg body weight, respectively), and then decapitated. The head was immediately put into ice cold Ringer's solution, which contained (in mM): NaCl 124, KCl 3, $MgSO_4$ 1.3, $CaCl_2$ 2, $NaHCO_3$ 26, NaH_2PO_4 1.25, glucose 15; pH 7.6 and 305 mOsm. The pH was kept at 7.4 by bubbling with 95% O_2 and 5% CO_2. The nose was dissected out *en bloc*. The MOE attached to the nasal septum and the dorsal recess was removed and kept in oxygenated Ringer. Immediately before starting the recording session, the entire MOE was peeled away from the underlying bone and transferred to a recording chamber with the mucus layer facing up. Oxygenated Ringer was continuously perfused at room temperature.

The dendritic knobs of OSNs were visualized with an upright microscope (Olympus BX51WI) equipped with an Olympus DP72 camera and a 40× water-immersion objective. An extra 2× magnification was obtained by a magnifying lens in the light path. In β2AR→M71-GFP mice, the GFP+ OSNs were visualized under fluorescent illumination. Superimposition of the fluorescent and bright-field images allowed identification of the fluorescent cells under bright field, which directed the recording pipettes. In wild-type C57BL/6 mice, OSNs were recorded randomly using bright-field illumination. Electrophysiological recordings were controlled by an EPC-10 USB amplifier combined with Patchmaster software (HEKA Electronic, Germany). Perforated patch clamp was performed on the dendritic knobs by including 260 μM nystatin in the recording pipette, which was filled with the following solution (in mM): KCl 70, KOH 53, methanesulfonic acid 30, EGTA 5, HEPES 10, sucrose 70; pH 7.2 (KOH) and 310 mOsm. The junction potential was ~9 mV and was corrected in all experiments off-line. Under voltage-clamp mode, the signals were filtered at 10 kHz followed by 2.9 kHz, and sampled at 20 kHz.

A seven-barrel pipette was used to deliver stimuli by pressure ejection through a picospritzer (Pressure System IIe, Toohey Company, Fairfield, NJ). The stimulus electrode was placed ~20 μm downstream from

the recording site. Distance and pressure were adjusted in order to minimize mechanical responses (Grosmaitre et al., 2007). All stimuli were delivered at a 138 kPa (~20 psi) pressure indicated on the picospritzer, with a 500 ms pulse length. Isoproterenol HCl (Tocris, Lille, France) was prepared in 1 M stock solution in water and kept at −20 °C; final solutions were prepared before each experiment by adding Ringer. The odorant mixture consists of 19 compounds in equal molar concentration (Grosmaitre et al., 2009): heptanol, octanol, hexanal, heptanal, octanal, heptanoic acid, octanoic acid, cineole, amyl acetate, (+) limonene, (−) limonene, (+) carvone, (−) carvone, 2-heptanone, anisaldehyde, benzaldehyde, acetophenone, 3-heptanone, and ethyl vanillin. Odorant mixture was prepared as a 0.1 M solution in DMSO and kept at −20 °C; final solutions at 10^{-5} M for each odorant were prepared before each experiment by adding Ringer. Forskolin, an activator of adenylyl cyclase, was prepared as a 10 mM stock solution in DMSO. IBMX, an inhibitor of phosphodiesterases, was prepared as a 100 mM stock solution in DMSO. Final solution containing 200 μM of IBMX and 20 μM of forskolin was prepared before each experiment by adding Ringer. All chemicals were obtained from Sigma-Aldrich unless otherwise stated.

Data were analyzed using Fitmaster (HEKA). Maximum amplitude of the response and kinetics characteristics were measured. Dose–response curves were drafted and fitted using Origin software (OriginLabs).

Acknowledgments

We thank Brian Kobilka for providing β1AR-KO mice and β2AR-KO mice; Paul Feinstein for construction of the targeting vector and Wei Tang for blastocyst injections at The Rockefeller University; and Tobias Burbach for technical assistance. This work was supported by the National Institutes of Health (M.M. and P.M.); the Max Planck Society and European Research Council Advanced Grant ORGENECHOICE (P.M.); and CNRS and the Conseil Régional de Bourgogne (X.G.).

References

Aoki, M., Takeuchi, H., Nakashima, A., Nishizumi, H., Sakano, H., 2013. Possible roles of Robo1+ ensheathing cells in guiding dorsal-zone olfactory sensory neurons in mouse. Dev. Neurobiol 73, 828–840.
Araneda, R.C., Firestein, S., 2006. Adrenergic enhancement of inhibitory transmission in the accessory olfactory bulb. J. Neurosci. 26, 3292–3298.
Barnea, G., O'Donnell, S., Mancia, F., Sun, X., Nemes, A., Mendelsohn, M., Axel, R., 2004. Odorant receptors on axon termini in the brain. Science 304, 1468.
Belluscio, L., Gold, G.H., Nemes, A., Axel, R., 1998. Mice deficient in G_{olf} are anosmic. Neuron 20, 69–81.
Bozza, T., Feinstein, P., Zheng, C., Mombaerts, P., 2002. Odorant receptor expression defines functional units in the mouse olfactory system. J. Neurosci. 22, 3033–3043.
Buck, L., Axel, R., 1991. A novel multigene family may encode odorant receptors: a molecular basis for odor recognition. Cell 65, 175–187.
Bush, C.F., Hall, R.A., 2008. Olfactory receptor trafficking to the plasma membrane. Cell. Mol. Life Sci. 65, 2289–2295.
Bush, C.F., Jones, S.V., Lyle, A.N., Minneman, K.P., Ressler, K.J., Hall, R.A., 2007. Specificity of olfactory receptor interactions with other G-protein coupled receptors. J. Biol. Chem. 282, 19042–19051.
Chruscinski, A.J., Rohrer, D.K., Schauble, E., Desai, K.H., Bernstein, D., Kobilka, B.K., 1999. Targeted disruption of the β2 adrenergic receptor gene. J. Biol. Chem. 274, 16694–16700.
Ennis, M., Zhou, F.M., Ciombor, K.J., Aroniadou-Anderjaska, V., Hayar, A., Borrelli, E., Zimmer, L.A., Margolis, F., Shipley, M.T., 2001. Dopamine D2 receptor-mediated presynaptic inhibition of olfactory nerve terminals. J. Neurophysiol. 86, 2986–2997.
Feinstein, P., Mombaerts, P., 2004. A contextual model for axonal sorting into glomeruli in the mouse olfactory system. Cell 117, 817–831.
Feinstein, P., Bozza, T., Rodriguez, I., Vassalli, A., Mombaerts, P., 2004. Axon guidance of mouse olfactory sensory neurons by odorant receptors and the β2 adrenergic receptor. Cell 117, 833–846.
Grosmaitre, X., Vassalli, A., Mombaerts, P., Shepherd, G.M., Ma, M., 2006. Odorant responses of olfactory sensory neurons expressing the odorant receptor MOR23: a patch clamp analysis in gene-targeted mice. Proc. Natl. Acad. Sci. U. S. A. 103, 1970–1975.
Grosmaitre, X., Santarelli, L.C., Tan, J., Luo, M., Ma, M., 2007. Dual functions of mammalian olfactory sensory neurons as odor detectors and mechanical sensors. Nat. Neurosci. 10, 348–354.
Grosmaitre, X., Fuss, S.H., Lee, A.C., Adipietro, K.A., Matsunami, H., Mombaerts, P., Ma, M., 2009. SR1, a mouse odorant receptor with an unusually broad response profile. J. Neurosci. 29, 14545–14552.
Hague, C., Uberti, M.A., Chan, Z., Bush, C.F., Jones, S.V., Ressler, K.J., Hall, R.A., Minneman, K.P., 2004. Olfactory receptor surface expression is driven by association with the β2-adrenergic receptor. Proc. Natl. Acad. Sci. U. S. A. 101, 13672–13676.
Hegg, C.C., Lucero, M.T., 2004. Dopamine reduces odor- and elevated-K^+-induced calcium responses in mouse olfactory receptor neurons in situ. J. Neurophysiol. 91, 1492–1499.
Ishii, T., Mombaerts, P., 2008. Expression of nonclassical class I major histocompatibility genes defines a tripartite organization of the mouse vomeronasal system. J. Neurosci. 28, 2332–2341.
Ishii, T., Omura, M., Mombaerts, P., 2004. Protocols for two- and three-color fluorescent RNA in situ hybridization of the main and accessory olfactory epithelia in mouse. J. Neurocytol. 33, 657–669.
Jones, D.T., Reed, R.R., 1989. G_{olf}: an olfactory neuron specific-G protein involved in odorant signal transduction. Science 22, 790–795.
Kawai, F., Kurahasahi, T., Kaneko, A., 1999. Adrenaline enhances odorant contrast by modulating signal encoding in olfactory receptor cells. Nat. Neurosci. 2, 133–138.
Khan, M., Vaes, E., Mombaerts, P., 2011. Regulation of the probability of mouse odorant receptor gene choice. Cell 147, 907–921.
Khan, M., Vaes, E., Mombaerts, P., 2013. Temporal patterns of odorant receptor gene expression in adult and aged mice. Mol. Cell. Neurosci. http://dx.doi.org/10.1016/j.mcn.2013.08.001.
Kobilka, B., 2013. The structural basis of G-protein coupled receptor signaling (Nobel lecture). Angew. Chem. Int. Ed. Engl. 52, 6380–6388.
Koster, N.L., Norman, A.B., Richtand, N.M., Nickell, W.T., Puche, A.C., Pixley, S.K., Shipley, M.T., 1999. Olfactory receptor neurons express D2 dopamine receptors. J. Comp. Neurol. 411, 666–673.
Lam, R., Mombaerts, P., 2013. Odorant responsiveness of embryonic mouse olfactory sensory neurons expressing the odorant receptors S1 or MOR23. Eur. J. Neurosci. 38, 2210–2217.
Lee, A.C., He, J., Ma, M., 2011. Olfactory marker protein is critical for functional maturation of olfactory sensory neurons and development of mother preference. J. Neurosci. 31, 2974–2982.
Lefkowitz, R.J., 2013. A brief history of G-protein coupled receptors (Nobel lecture). Angew. Chem. Int. Ed. Engl. 52, 6380–6388.
Li, Y.R., Matsunami, H., 2011. Activation state of the M3 muscarinic acetylcholine receptor modulates mammalian odorant receptor signaling. Sci. Signal. 4, ra1.
Liu, H.Y., Wenzel-Seifert, K., Seifert, R., 2001. The olfactory G protein $G_{\alpha olf}$ possesses a lower GDP-affinity and deactivates more rapidly than $G_{s\alpha short}$: consequences for receptor-coupling and adenylyl cyclase activation. J. Neurochem. 78, 325–338.
Ma, M., Chen, W.R., Shepherd, G.M., 1999. Electrophysiological characterization of rat and mouse olfactory receptor neurons from an intact epithelial preparation. J. Neurosci. Methods 92, 31–40.
Mombaerts, P., Wang, F., Dulac, C., Chao, S.K., Nemes, A., Mendelsohn, M., Edmondson, J., Axel, R., 1996. Visualizing an olfactory sensory map. Cell 87, 675–686.
Nakashima, A., Takeuchi, H., Imai, T., Saito, H., Kiyonari, H., Abe, T., Chen, M., Weinstein, L.S., Yu, C.R., Storm, D.R., et al., 2013. Agonist-independent GPCR activity regulates anterior–posterior targeting of olfactory sensory neurons. Cell 154, 1314–1325.
Nguyen, M.Q., Zhou, Z., Marks, C.A., Ryba, N.J.P., Belluscio, L., 2007. Prominent roles for odorant receptor coding sequences in allelic exclusion. Cell 131, 1009–1017.
Okada, Y., Miyamoto, T., Toda, K., 2003. Dopamine modulates a voltage-gated calcium channel in rat olfactory receptor neurons. Brain Res. 968, 248–255.
Rodriguez, I., Feinstein, P., Mombaerts, P., 1999. Variable patterns of axonal projections of sensory neurons in the mouse vomeronasal system. Cell 97, 199–208.
Rohrer, D.K., Desai, K.H., Jasper, J.R., Stevens, M.E., Regula, D.P., Barsh, G.S., Bernstein, D., Kobilka, B., 1996. Targeted disruption of the mouse β1-adrenergic receptor gene: developmental and cardiovascular effects. Proc. Natl. Acad. Sci. U. S. A. 93, 7375–7380.
Sammeta, N., Yu, T.T., Bose, S.C., McClintock, T.S., 2007. Mouse olfactory sensory neurons express 10,000 genes. J. Comp. Neurol. 502, 1138–1156.
Strotmann, J., Levai, O., Fleischer, J., Schwarzenbacher, K., Breer, H., 2004. Olfactory receptor proteins in axonal processes of chemosensory neurons. J. Neurosci. 24, 7754–7761.
Vassalli, A., Rothman, A., Feinstein, P., Zapotocky, M., Mombaerts, P., 2002. Minigenes impart odorant receptor-specific axon guidance in the OB. Neuron 35, 681–696.